Chin. J. Mech. Eng. (2017) 30:888–899
DOI 10.1007/s10033-017-0102-8

ORIGINAL ARTICLE

# Kinematics and Path Following Control of an Articulated Drum Roller

**Yongming BIAN[1] · Meng YANG[1] · Xiaojun FANG[1] · Xiahui WANG[1]**

Received: 25 May 2016 / Revised: 29 August 2016 / Accepted: 9 October 2016 / Published online: 22 March 2017


**Abstract** Automatic navigation of an articulated drum roller, which is an articulated steering type vehicle widely used in the construction industry, is highly expected for operation cost reduction and improvement of work efficiency. In order to achieve the path following control, considering that its steering system is articulated steering and two frames are articulated by an active revolute joint, a kinematic model and an error dynamic state-space equation of an articulated drum roller are proposed. Besides, a state-feedback control law based on Lyapunov stability theory is also designed, which can be proved to achieve the purpose of control by the analysis of stability. What's more, to evaluate the performance of the proposed method, simulation under the MATLAB/Simulink and experiments using positioning algorithm and errors correction at the uneven construction site are performed, with initial displacement error (−1.5 m), heading error (−0.11 rad) and steering angle (−0.19 rad). Finally, simulation and experimental results show that the errors and steering angle can decrease gradually, and converge to zero with time. Meanwhile, the control input is not saturated. An articulated drum roller can lock into a desired path with the proposed method in uneven fields.

Supported by National Key Technology Support Program of China (Grant No. 2015BAF07B05), and Fundamental Research Funds for the Central Universities of China.

✉ Meng YANG
stek_young@163.com

[1] School of Mechanical Engineering, Tongji University, Shanghai 201804, China

**Keywords** Kinematics · Path following control · Articulated drum roller · Positioning algorithm · Positioning errors correction

## 1 Introduction

The past two decades have witnessed an increase in the use of positioning and navigation technologies in land vehicle applications to improve safety and handling characteristics, including automated car navigation, emergency assistance, agricultural machinery, engineering machinery and so on [1, 2]. Automatic navigation of an articulated steering type vehicle such as a drum roller, which is widely used for constructing dams, airports and roads, is also highly expected for operation cost reduction and improvement of work efficiency. What's more, it also makes one operate multi-machines performance possible in large-scale construction.

An articulated steering type vehicle has two frames (front and rear) and they are articulated by an active revolute joint. Its steering action can be achieved by changing the angle between the front and rear frames. For the real vehicle working at the construction site, this is normally done by two hydraulic cylinders between the two frames, the length of which can be controlled. The structural features and the extra degrees of freedom caused by joint weaken the lateral stiffness of an articulated steering type vehicle, resulting in a poor performance during the straight-line driving and increasing the difficulty in control [3].

Automatic navigation is mainly based on two techniques: positioning and control [4–7]. Control laws for automatic navigation can be developed by modeling the vehicle with a kinematic model [8–11]. There are many studies on a tractor-trailer, which has a similar mechanical

structure with an articulated steering vehicle. The kinematic model, steering limitations and controllability of a tractor-trailer using differential geometric tools have been reviewed and discussed [12–14]. YOSHIMOTO, et al [15], proposed a closed- loop control method of backward movement using the path following method for an unmanned vehicle with a trailer for operation in an orchard. YANG, et al [16], proposed a control framework relying on mixed logical dynamics hybrid modeling and model predictive control method to achieve the path tracking control for the backing-up tractor-trailer system. KHALAJI, et al [17], designed a kinematic control law based on switching control method and a non-model-based dynamic control law to stabilize the tractor-trailer wheeled robot about a desired configuration. HUYNH, et al [18], designed a controller for tracking straight-line and circular paths by combining nonlinear proportional-integral control with the backstepping control. TIAN, et al [19], proposed a four degrees of freedom single track model of a tractor-trailer and studied the influences of the structural and operating parameters on the vehicle. However, the tractor and trailer is articulated by a passive revolute joint, the control of a tractor-trailer depends on how the trailer moves respective to the tractor. Besides, the steering instantaneous center of the tractor is not coincident with that of the trailer, it is best to consider the two objects as separate pieces with an angular relationship. Therefore, the kinematic model of an articulated steering type vehicle is different from the one of a tractor-trailer and the control laws also can not be used for an articulated steering type vehicle directly.

There are also several studies on an articulated steering type vehicle. YAMAKAWA, et al [20], studied on turning characteristics of an articulated tracked vehicle. ALSHAER, et al [21], proposed a path planning methodology for an articulated large wheel loader drawing a V-shape path and designed a PID controller to keep machine lateral position within the pre-defined path while traveling with constant speed. NAYL, et al [22], proposed an on-line path planning algorithm producing on-line the next reference waypoint and a Model Predictive Controller utilized for creating the proper control signal. They also analyzed the effect of kinematic parameters of the path planning algorithm in Ref. [23]. SHIROMA, et al [24], introduced another virtual velocity constraint and formulated nonlinear state equations using two constraints, but the nonlinear state-feedback controller was designed still using the exact linearization method. RAINS, et al [25], studied a pure-pursuit navigational algorithm, based on a predetermined look-ahead distance, to compute the appropriate turning radius to achieve the desired look-ahead coordinate. Mobile robots which explore untraditional environments are center-articulated, and their kinematic model resembles articulated-steering vehicles. DELROBAEI, et al [26], investigated a kinematic model for center-articulated mobile robots, and proposed a feedback method to control a parking maneuver using a beacon-based positioning system. However, although these papers propose different control methods for path following, they do not consider the control input saturation. KOU, et al [27], showed that the control input saturation should be taken into account when studying on the path tracking problem of the articulated vehicle, due to the limited steering angle and its velocity produced by the hydraulic actuators. What's more, the existing studies use only simulations and experiments when the prototype or vehicle exists in ideal environments.

This paper aims to realize the path following control of an articulated drum roller, which is also an articulated steering type vehicle. A kinematic model of the articulated drum roller purely from geometric consideration of the vehicle and its velocity constraints, and a linear mathematical error dynamic state-space equation were proposed firstly. Then, a state-feedback control law was proposed to follow a desired straight line based on Lyapunov stability theory and relying on the linear error dynamics state-space equation, which can be proved to achieve the purpose of control by the analysis of stability. Considering that the main working device of an articulated drum roller is the roller drum of front frame while the GPS receiver is placed in the driver's cab of rear frame generally, a method was proposed to calculate the position and orientation of the roller drum from the GPS receiver position and the kinematic model, which contributes to obtain a more precise positioning. Besides, a two- dimensional tilt sensor was used to reduce the GPS positioning errors resulting from the tilt of front and rear frames during the process of moving on the rough fields, which cause the path following controlling errors and affect the experimental results. To evaluate the performance of the proposed method, simulation under the MATLAB/Simulink and experiments using positioning algorithm and errors correction at the construction site were performed, with initial displacement error ($-1.5$ m), heading error ($-0.11$ rad) and steering angle ($-0.19$ rad). Finally, the simulation and experimental results show that the errors and steering angle can decrease gradually, and converge to zero with time. Meanwhile, the control input is not saturated. With the path following method, the articulated drum roller can lock onto a desired path in uneven fields and the only input is the angle velocity of steering. In other words, it is possible to achieve control using only a small number of control inputs.

## 2 Articulated Drum Roller Modeling

### 2.1 Kinematic Model

First, the kinematic model of an articulated drum roller, which has front-wheel steering and the rear wheels are

forward-driven without being steered, is being described. As depicted in Fig. 1, where $O-XY$ is the Cartesian coordinate;$\theta_P$ is the orientation of the roller drum of the front frame with respect to the positive X-axis;$\delta$ is the steering angle of the roller drum with respect to the forward direction of the vehicle;$P(x_P, y_P)$ is the center position of the roller drum axle of the front frame in the Cartesian coordinate;$L_1$ is the distance between the junction point $H$ and the roller drum axle;$v_P$ is the forward velocity of the roller drum;$\theta_Q$ is the orientation of the rear frame with respect to the positive X-axis;$Q(x_Q, y_Q)$ is the center position of the rear wheel axle of the vehicle in the Cartesian coordinate;$L_2$ is the distance between the junction point $H$ and the rear wheel axle;$v_Q$ is the forward velocity of the rear frame.

Here, for deriving the vehicle's kinematic equations, it is assumed that the steering angle $\delta$ remains constant under small displacement and the vehicle moves on a plane without slipping effects, the velocity is limited within the maximum allowed velocity, which prevents the vehicle from slipping. By examining the vehicle's depicted geometrical characteristics, it can be easily derived that

$$\begin{aligned} \dot{x}_P &= v_P \cos\theta_P, \\ \dot{y}_P &= v_P \sin\theta_P, \end{aligned} \tag{1}$$

Since the junction point $H$ is common to both the front and rear frames of the vehicle, then

$$\boldsymbol{v_P} + \dot{\theta}_P \times \boldsymbol{PH} = \boldsymbol{v_Q} + \dot{\theta}_Q \times \boldsymbol{QH}, \tag{2}$$

where $\dot{\theta}_P$ and $\dot{\theta}_Q$ are the angular velocities of the front and rear frames respectively.

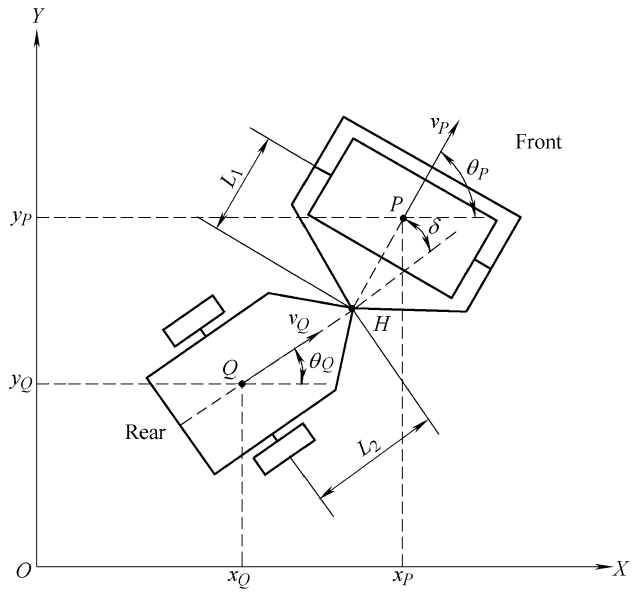


**Fig. 1** Articulated drum roller schematic and description of variables

Hence, the velocities $v_P$ and $v_Q$ are considered to have the same changing law with respect to the velocity of the junction point $H$, and the relative velocity vector equations can be defined as

$$\begin{pmatrix} v_P \\ 0 \end{pmatrix} + \begin{pmatrix} 0 \\ -L_1\dot{\theta}_P \end{pmatrix} = \begin{pmatrix} v_Q \cos\delta \\ -v_Q \sin\delta \end{pmatrix} + \begin{pmatrix} L_2\dot{\theta}_Q \sin\delta \\ L_2\dot{\theta}_Q \cos\delta \end{pmatrix}. \tag{3}$$

By using the geometric relationship

$$\theta_Q = \theta_P - \delta, \tag{4}$$

the angle velocity $\dot{\theta}_P$ of the roller drum of the front frame is

$$\dot{\theta}_P = \frac{v_P \sin\delta + L_2\dot{\delta}}{L_2 + L_1\cos\delta}. \tag{5}$$

The values of corresponding angle velocities for the front and rear frames, which are being defined as $\dot{\theta}_P$ and $\dot{\theta}_Q$ respectively, are different when $L_1 \neq L_2$ or the vehicle is not driving straight $(\delta \neq 0)$ according to Eq. (3). Finally, the angle velocity of the rear frame is being derived from Eq. (4) as $\dot{\theta}_Q = \dot{\theta}_P - \delta$, or

$$\dot{\theta}_Q = \frac{v_P \sin\delta - L_1\dot{\delta}\cos\delta}{L_2 + L_1\cos\delta}. \tag{6}$$

From the above, the kinematic model of the articulated drum roller is expressed as follows:

$$\begin{aligned} \dot{x}_P &= v_P \cos\theta_P, \\ \dot{y}_P &= v_P \sin\theta_P, \\ \dot{\theta}_P &= \frac{v_P \sin\delta + L_2\dot{\delta}}{L_2 + L_1\cos\delta}. \end{aligned} \tag{7}$$

### 2.2 Path Following Control Problem and Error Dynamic State-Space Equation

The path following control problem of an articulated drum roller is considered firstly, as it is depicted shown in Fig. 2, where $(x_R, y_R)$ is the center position of the roller drum axle;$\theta_R$ is the orientation and $v_R$ is the forward velocity of the reference vehicle.

The kinematic model of the reference vehicle is expressed in the same form as that of the real vehicle:

$$\begin{aligned} \dot{x}_R &= v_R \cos\theta_R, \\ \dot{y}_R &= v_R \sin\theta_R, \\ \dot{\theta}_R &= \omega_R. \end{aligned} \tag{8}$$

By transforming the Cartesian coordinate into the vehicle-based coordinate, the relative errors between real vehicle and reference vehicle is defined as follows:

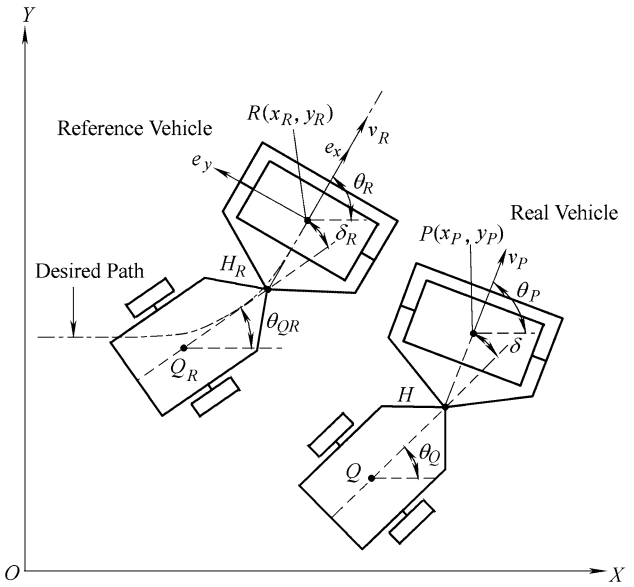


**Fig. 2** Path following control problem

$$\begin{pmatrix} e_x \\ e_y \\ e_\theta \end{pmatrix} = \begin{pmatrix} \cos\theta_R & \sin\theta_R & 0 \\ -\sin\theta_R & \cos\theta_R & 0 \\ 0 & 0 & 1 \end{pmatrix} \begin{pmatrix} x_P - x_R \\ y_P - y_R \\ \theta_P - \theta_R \end{pmatrix}, \tag{9}$$

where $e_x$ is the error in the longitudinal direction;$e_y$ is the error in the lateral direction;$e_\theta$ is the heading error.

From Eq. (9), the error dynamic is

$$\begin{pmatrix} \dot{e}_x \\ \dot{e}_y \\ \dot{e}_\theta \end{pmatrix} = \begin{pmatrix} \omega_R e_y - v_R + v_P \cos e_\theta \\ v_P \sin e_\theta - \omega_R e_x \\ \dot{\theta}_P - \omega_R \end{pmatrix}. \tag{10}$$

In order to treat the tracking control problem as a path following control problem, the error in the longitudinal direction is not considered, and the error in the lateral direction $e_y$ is defined as the displacement error. Therefore, it needs to be satisfied that $e_x = 0$ and $\dot{e}_x = 0$. Then, according to the track parameters geometric relationship, the following relationships hold:

$$\omega_R = \frac{v_P \cos e_\theta}{r_P - e_y} = \rho \frac{v_P \cos e_\theta}{1 - e_y \rho}, \tag{11}$$

$$v_R = \frac{v_P \cos e_\theta}{1 - e_y \rho}, \tag{12}$$

where $r_P$ is the turning radius of the real vehicle;$\rho$ is the curvature defined as $\rho = 1/r_P$.

In straight-line path following control, the assumption has been made that $e_\theta$ and $\delta$ is a small angle measured in radians, and the curvature $\rho = 1/r_P = 0$.

Finally, the linear state-space equation for the articulated drum roller is expressed as follows:

$$\begin{pmatrix} \dot{e}_y \\ \dot{e}_x \\ \dot{\delta} \end{pmatrix} = \begin{pmatrix} 0 & v_P & 0 \\ 0 & 0 & \frac{v_P}{L_1 + L_2} \\ 0 & 0 & 0 \end{pmatrix} \begin{pmatrix} e_y \\ e_\theta \\ \delta \end{pmatrix} + \begin{pmatrix} 0 \\ \frac{L_2}{L_1 + L_2} \\ 1 \end{pmatrix} \dot{\delta}. \tag{13}$$

The purpose of the control is to make the drum roller move along the desired path. In other words, the purpose of control is expressed as follows:

$$\begin{aligned} e_y &= 0, \\ e_\theta &= 0, \\ \delta &= 0. \end{aligned} \tag{14}$$

## 3 Path Following Control

### 3.1 Design of Control Law

Analysis of the state-space equation shows that the state of the drum roller is controllable, using the input $\dot{\delta}$. Besides, all three of the state variables can be measured or calculated directly, automatic control of the path following can be achieved using state variable feedback.

The Lyapunov stability theory [28, 29] is a common tool to design control laws. Here, a control law based on the Lyapunov stability theory and relying on the state-space equation in Cartesian coordinate is being designed, which drives the articulated drum roller from any initial condition $(e_y, e_\theta, \delta)$ to the final condition $(0, 0, 0)$.

First, a positive definite Lyapunov function candidate is chosen as follows:

$$V = \frac{1}{2} K_1 e_y^2 + \frac{1}{2} e_\theta^2, \tag{15}$$

where $K_1$ is an arbitrary constant and $K_1 > 0$.

Then, the time derivative of Eq. (15) is calculated as

$$\dot{V} = K_1 e_y \dot{e}_y + e_\theta \dot{e}_\theta. \tag{16}$$

Substituting Eq. (13) into Eq. (16) gives

$$\dot{V} = e_\theta \left( K_1 v_P e_y + \frac{v_P}{L_1 + L_2} \delta + \frac{L_2}{L_1 + L_2} \dot{\delta} \right). \tag{17}$$

If the control input is chosen as

$$\dot{\delta} = -\frac{K_1 v_P (L_1 + L_2)}{L_2} e_y - \frac{K_2 (L_1 + L_2)}{L_2} e_\theta - \frac{v_P}{L_2} \delta, \tag{18}$$

then $\dot{V}$ is negative definite as

$$\dot{V} = -K_2 e_\theta^2 \leq 0, \tag{19}$$

where $K_2$ is an arbitrary positive constant.$\dot{V} \leq 0$ implies stability of the system states. Convergence (asymptotic stability) depends on the choice of $K_1$ and $K_2$, as discussed next.

### 3.2 Stability Analysis

The proposed Lyapunov function candidate $V$ is lower bounded and $\dot{V}$ is negative definite. From Eqs. (15) and (19), $e_y$ and $e_\theta$ are shown to be bounded. Because $v_P$ and $\delta$ are bounded in physical world,$\dot{\delta}$ is also bounded from Eq. (18). The time derivative of Eq. (19) is calculated as shown in the following expression:

$$\ddot{V} = -2K_2 e_\theta \left( \frac{v_P}{L_1 + L_2}\delta + \frac{L_2}{L_1 + L_2}\dot{\delta} \right). \tag{20}$$

Due to the boundedness of the state variables and control input, $\ddot{V}$ gets bounded, so $\dot{V}$ is uniformly continuous, and $\dot{V} \to 0$ as $t \to \infty$ holds from Barbalat's lemma [29]. In other words, $e_\theta \to 0$ as $t \to \infty$ holds. Then, from Eqs. (13) and (18), the time derivative of $\dot{e}_\theta$ is calculated as shown in the following expression:

$$\begin{aligned} \ddot{e}_\theta &= -K_1 \dot{v}_P e_y - K_1 v_P \dot{e}_y - K_2 \dot{e}_\theta \\ &= -K_1 \dot{v}_P e_y - K_1 v_P^2 e_\theta - K_2 \left( \frac{v_P}{L_1 + L_2}\delta + \frac{L_2}{L_1 + L_2}\dot{\delta} \right), \end{aligned} \tag{21}$$

$\dot{v}_P$ is bounded in physical world, so $\ddot{e}_\theta$ gets bounded. Therefore, the following is derived from Barbalat's lemma:

$$\lim_{t\to\infty} \dot{e}_\theta = \frac{v_P}{L_1 + L_2}\delta + \frac{L_2}{L_1 + L_2}\dot{\delta} = 0. \tag{22}$$

Then, $\dot{\delta}$ is calculated as

$$\dot{\delta} = -\frac{v_P}{L_2}\delta. \tag{23}$$

Here, a candidate of the positive definite Lyapunov function $V_\delta$ is chosen as follows:

$$V_\delta = \frac{1}{2}\delta^2. \tag{24}$$

The time derivative of Eq. (24) is calculated as

$$\dot{V}_\delta = -\frac{v_P}{L_2}\delta^2 \le 0. \tag{25}$$

Thus, the time derivative of Eq. (25) is calculated as

$$\ddot{V}_\delta = -\frac{\dot{v}_P}{L_2}\delta^2 - \frac{2v_P^2}{L_2^2}\delta^2. \tag{26}$$

From Eq. (26),$\ddot{V}_\delta$ is shown to be bounded, and $\dot{V}_\delta$ is uniformly continuous. From Barbalat's lemma,$\dot{V}_\delta \to 0$ as $t \to \infty$ holds. In other words, $\delta \to 0$ as $t \to \infty$ holds and $\dot{\delta} \to 0$ as $t \to \infty$ holds when the articulated vehicle moves forward on the straight. From Eq. (18), $e_y \to 0$ as $t \to \infty$ holds when $v_P \neq 0$. Consequently, the purpose of path following control is achieved with the designed control law of Eq. (18).

## 4 Positioning System

### 4.1 Position and Orientation Computation of the Roller Drum Axle Midpoint from GPS Position

In order to achieve path following control based on control law described in Eq. (18), feedback from the states of the roller drum, including position and orientation, is needed. In this article, this information is obtained from the GPS receiver finally, which is placed on the driver's cab as shown in Fig. 3.

In order to improve the positioning precision, the position and orientation of the roller drum axle midpoint is computed from GPS data together with the kinematic model.

First, the position $(x_P, y_P)$ at the midpoint of the roller drum axle is obtained from junction point $H(x_H, y_H)$ from geometric relationship as shown in Fig. 4.

The geometric relationship between $(x_P, y_P)$ and $(x_H, y_H)$ is

$$\begin{aligned} x_H &= x_P - L_1 \cos\theta_P, \\ y_H &= y_P - L_1 \sin\theta_P. \end{aligned} \tag{27}$$

Then, the time derivative of Eq. (27) is calculated as

$$\begin{aligned} \dot{x}_H &= \dot{x}_P + L_1\dot{\theta}_P \sin\theta_P = v_P \cos\theta_P + L_1\dot{\theta}_P \sin\theta_P, \\ \dot{y}_H &= \dot{y}_P - L_1\dot{\theta}_P \cos\theta_P = v_P \sin\theta_P - L_1\dot{\theta}_P \cos\theta_P. \end{aligned} \tag{28}$$

From Eqs. (1) and (28):

$$\begin{aligned} &\dot{x}_H^2 + \dot{y}_H^2 \\ &= (v_P \cos\theta_P + L_1\dot{\theta}_P \sin\theta_P)^2 \\ &+ (v_P \sin\theta_P - L_1\dot{\theta}_P \cos\theta_P)^2 \\ &= v_P^2 + L_1^2\dot{\theta}_P^2, \end{aligned} \tag{29}$$

and then,$\dot{\theta}_P$ is calculated from Eq. (29) as shown in the following expression:

$$\dot{\theta}_P = \pm\frac{1}{L_1}\sqrt{\dot{x}_H^2 + \dot{y}_H^2 - v_P^2}. \tag{30}$$


**Fig. 3** GPS receiver position on the driver's cab

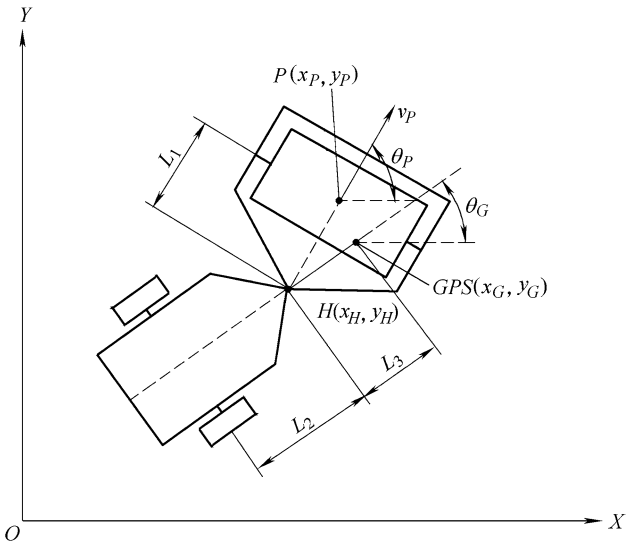


**Fig. 4** The geometric relationship among $P(x_P, y_P)$, $H(x_H, y_H)$, $GPS(x_G, y_G)$

Next, the position $(x_H, y_H)$ at the junction point $H$ is obtained from the GPS receiver $(x_G, y_G, \theta_G)$ from geometric relationship as shown in Fig. 4.

The geometric relationship between $(x_H, y_H)$ and $(x_G, y_G, \theta_G)$ is

$$\begin{aligned} x_H &= x_G - L_3 \cos\theta_G, \\ y_H &= y_G - L_3 \sin\theta_G, \end{aligned} \tag{31}$$

where $L_3$ is the distance between the GPS receiver position and the junction point $H$, and $\theta_G$ is the orientation of the GPS receiver, which is also equal to the current $\theta_G$ according to the geometric relationship.

Then, the position of junction point $H$ can be obtained from the GPS receiver position, and the position and orientation of the roller drum can be obtained in a recursive way using the position at the junction point $H$ and the previous roller drum state, as follows:

$$x_H[n] = x_G[n] - L_3 \cos(\theta_G[n]), \tag{32}$$

$$y_H[n] = y_G[n] - L_3 \sin(\theta_G[n]), \tag{33}$$

$$\theta_P[n] = \theta_P[n-1] \pm \frac{\Delta T}{L_1}\sqrt{\left(\frac{x_H[n]-x_H[n-1]}{\Delta T}\right)^2 + \left(\frac{y_H[n]-y_H[n-1]}{\Delta T}\right)^2 - v_P^2}, \tag{34}$$

$$x_P[n] = x_P[n-1] + v_P \Delta T \cos(\theta_P[n]), \tag{35}$$

$$y_P[n] = y_P[n-1] + v_P \Delta T \sin(\theta_P[n]). \tag{36}$$

Eqs. (32)–(36) must be sequentially computed at each new GPS position, where $\Delta T$ is the time between the reception of two GPS positions.

### 4.2 Positioning Errors Correction

In practice, due to the rough fields, the front and rear frames of drum roller tilt inevitably during the process of moving. The degree of tilt is expressed by roll angle and pitch angle, and they can be up to 0.35 rad in general. If the GPS receiver is placed 3m above the ground, the maximum horizontal positioning errors in vehicle-based coordinates caused by roll angle will be 1.03 m, which has a serious effect on GPS positioning.

In order to correct the GPS positioning errors caused by the tilt of front and rear frames, a two-dimensional tilt sensor should be used to obtain the roll angle and pitch angle to calculate the horizontal and longitudinal positioning errors in vehicle-based coordinates.

Taking geometrical relationship into account:

$$\begin{aligned} e'_{tx} &= L_G \sin\alpha_x, \\ e'_{ty} &= L_G \sin\alpha_y, \end{aligned} \tag{37}$$

where $e'_{tx}$ is the longitudinal positioning error,$e'_{ty}$ is the horizontal positioning error,$\alpha_x$ is the pitch angle,$\alpha_y$ is the roll angle in vehicle-based coordinates and $L_G$ is the height of GPS receiver.

By transforming the vehicle-based coordinate into the Cartesian coordinate, from Eq. (37), it is derived that:

$$\begin{aligned} e_{tx} &= e'_{tx}\cos\theta_R + e'_{ty}\sin\theta_R, \\ e_{ty} &= -e'_{tx}\sin\theta_R + e'_{ty}\cos\theta_R, \end{aligned} \tag{38}$$

where $e_{tx}$ is the longitudinal positioning error and $e_{ty}$ is the horizontal positioning error in Cartesian coordinates.

Then, $e_{tx}$ and $e_{ty}$ can be used to correct the GPS position.

## 5 Simulation

### 5.1 Modeling

To evaluate the performance of the proposed path following control law, some simulation results are being presented. In the proposed control law, it is assumed that the error dynamic states have been measured directly or calculated, including the displacement error, heading error and steering angle. The controller action is the rate of steering angle which constraints on the control inputs, the states of the vehicle's error dynamic states. The overall block diagram of the proposed path following control is depicted in Fig. 5.

### 5.2 Simulation Results

For simulating the effectiveness of the proposed control law for the problem of path following for an articulated

drum roller, the following vehicle's characteristics have been considered:$L_1 = 1.5$ m, $L_2 = 1.76$ m, the velocity of the roller drum $v_P$ is set as $v_P = 0.5$ (m·s$^{-1}$) which is practical velocity. The initial conditions are the initial displacement error $e_y = -1.5$ m in Y-direction, the initial heading error $e_\theta = -0.11$ rad and the initial steering angle $\delta = -0.19$ rad. The steering angle (rad) is limited to $\delta \in [-0.611, 0.611]$ and the steering angle velocity (rad·s$^{-1}$) is limited to $\dot{\delta} \in [-0.2, 0.2]$ to follow the actual limits of a real articulated drum roller. The control gains used in the simulation are determined by tuning in experiments as $K_1 = 0.059$ and $K_2 = 0.202$. Above all, the simulation parameters of control system model are shown in Table 1.

The results of the path following simulation to the X-axis can be seen in Figs. 6, 7, 8, 9, 10. The parameters of the simulation results are shown in Table 2. Due to the initial condition, the drum roller adjusted quite sharply at the beginning. After about 5 s, the adjustment became smooth gradually. Finally, even though there were an initial displacement error (−1.5 m) in Y-direction, an initial heading error (−0.11 rad) and an initial steering angle (−0.19 rad), the vehicle converged to the X-axis as time goes by and $e_y, e_\theta, \delta$ and $\dot{\delta}$ became 0 after 30s. The Lyapunov function $V$ also became 0 as analyzed after 17 s. In conclusion, the effectiveness of the proposed control law for straight-line path following of the articulated vehicle is confirmed by the simulation results.

## 6 Experiments

### 6.1 Experimental Setup

A YZ26E articulated drum roller equipped with devices, as shown in Fig. 3, is used in the experiment. The drum roller is rear-wheel drive, and has vehicle control and status signals transmitted via a control area network (CAN). A EPEC 2023 vehicle controller is used to control the steering system and the speed of drum roller, as shown in Fig. 11(a). The steering angle is measured using a single-ring absolute encoder, transmitted via CANopen and offering up to 0.09 degrees accuracy with a resolution of 16

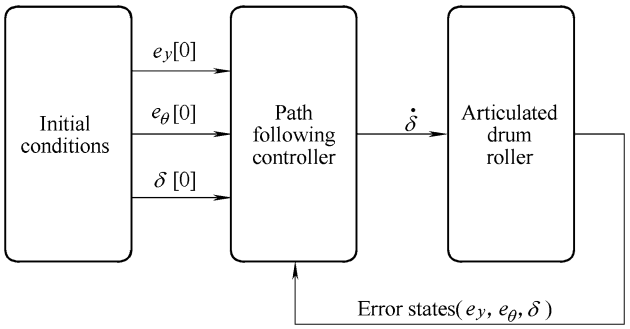


**Fig. 5** Overall block diagram of the proposed path following control

**Table 1** The simulation parameters of control system model

| Parameter | Value | Range | Description |
|---|---|---|---|
| $L_1$ /m | 1.5 | – | Length of *PH* |
| $L_2$ /m | 1.76 | – | Length of *QH* |
| $v_P$ /(m·s$^{-1}$) | 0.5 | – | Forward velocity |
| $e_y$ /m | −1.5 | – | Displacement error |
| $e_\theta$ /rad | −0.11 | – | Heading error |
| $\delta$ /rad | −0.19 | [−0.611, 0.611] | Steering angle |
| $\dot{\delta}$ /(rad·s$^{-1}$) | – | [−0.2,0.2] | Steering angle velocity |
| $K_1$ | 0.059 | – | Adjustment factor 1 |
| $K_2$ | 0.202 | – | Adjustment factor 2 |

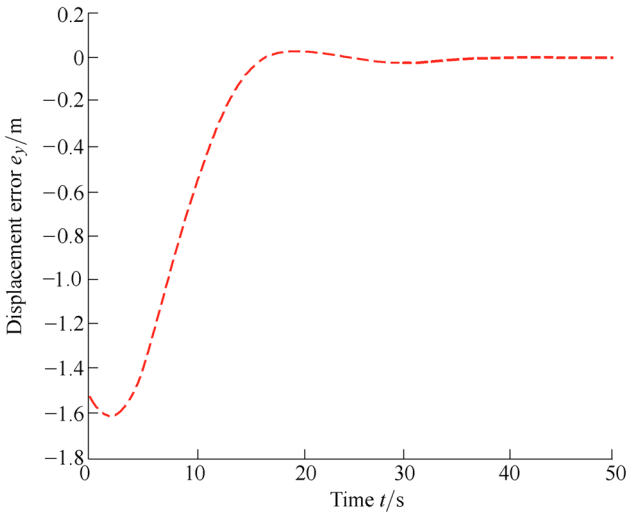


**Fig. 6** Simulation results of displacement error

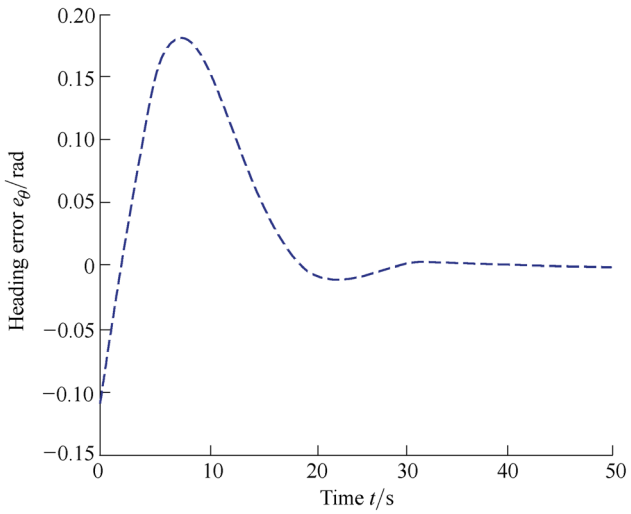


**Fig. 7** Simulation results of heading error

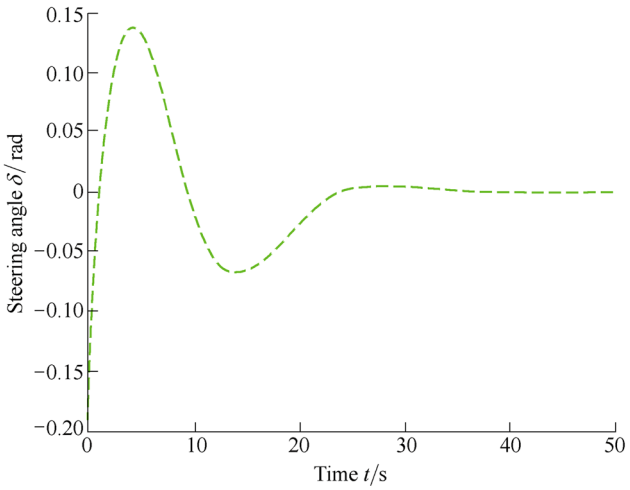


**Fig. 8** Simulation results of steering angle

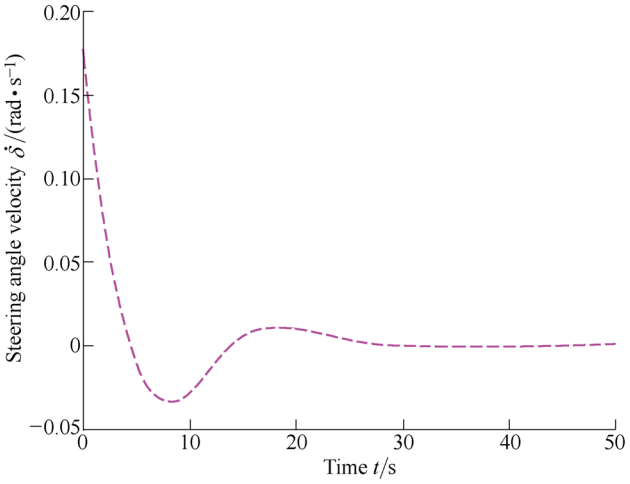


**Fig. 9** Simulation results of steering angle velocity

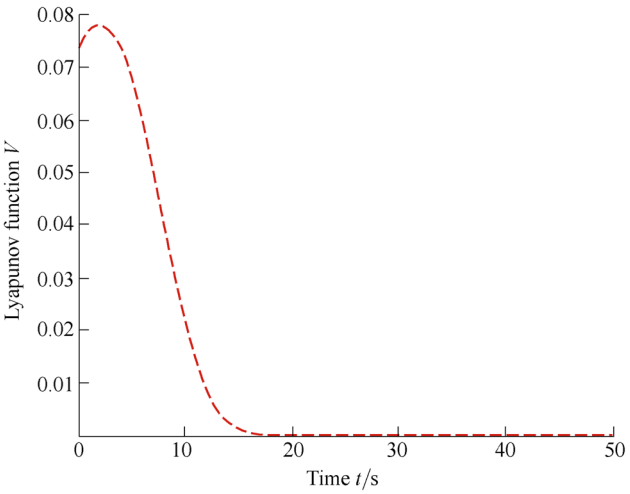


**Fig. 10** Simulation results of Lyapunov function

bits and $\delta$ is a small angle measured in radians, as shown in Fig. 11(b). State variables $e_y$ and $e_\theta$ are calculated by measuring the relative position and heading between the drum roller and desired path. The relative position and heading are measured using a Huace N71J GNSS receiver, which integrates a BD982 Trimble multi-mode multi-frequency motherboard and offers up to 0.008 m accuracy of horizontal and 0.015 m accuracy of vertical when working with carrier-phase measurements in Real Time Kinematic (RTK) mode, as shown in Fig. 11(c). A Huace N71 GNSS receiver configured to use RTK corrections is used as the reference station GPS, as shown in Fig. 11(d). Moreover, a 2-dimensional inclination tilt sensor is used to correct positioning error, connecting via CAN and offering up to 0.0017 rad accuracy with $\pm 0.7854$ rad measurement range, as shown in Fig. 11(c). The structure of experimental setup is shown in Fig. 12, and the experiment is performed at the construction site shown in Fig. 13.

### 6.2 Experimental Results and Discussion

An experiment was performed to evaluate the effectiveness of the proposed control law for the problem of path following for an articulated drum roller. The results of the path following experiment can be seen in Figs. 15, 16, 17, 18, 19. From Fig. 13, it can be observed that the field at the construction site is uneven. In addition, the roughness of experimental field $r_h$ can be calculated with the roll angle and pitch angle obtained by tilt sensor from geometric consideration of the vehicle, as shown in Fig. 14. Based on the longitudinal and horizontal roughness, the average roughness of the experimental field is about 0.11 m. There is no doubt that path following control on uneven road is more difficult than on flat road.

The results of the path following experiments can be seen in Figs. 15, 16, 17, 18, 19, which are quite similar with the simulation results. The parameters of the experimental results are shown in Table 3. From Tables 2–3, it is found that the difference between simulation results and experimental results is quite small, which is much higher than the accuracy of manual operation. From Figs. 15, 16, 17, it is found that errors and state variables converged to zero even if it was given initial conditions. Figures 17, 18 indicated that steering angle and input were not saturated. From Fig. 18, it was found that the value of $\dot{\delta}$ changed smoothly and it meant that the internal state of the system was stable.

Although the roughness of the experimental field is ignored in the simulation but not experiments, the tilt sensor used to correct the GPS position reduces the

**Table 2** Parameters of the simulation results

| Parameter | Peak value | Peak time/s | Trough value | Trough time/s | Zero time/s |
|---|---|---|---|---|---|
| Displacement error $e_y$ /m | 0.041 | 19 | −1.63 | 2 | 24 |
| Heading error $e_\theta$ /rad | 0.18 | 8 | −0.012 | 22 | 28 |
| Steering angle $\delta$ /rad | 0.13 | 5 | −0.068 | 14 | 35 |
| Steering angle velocity $\dot{\delta}$ /(rad·s$^{-1}$) | 0.01 | 19 | −0.032 | 8 | 29 |
| Lyapunov function $V$ | 0.078 | 2 | 0 | 16 | 16 |

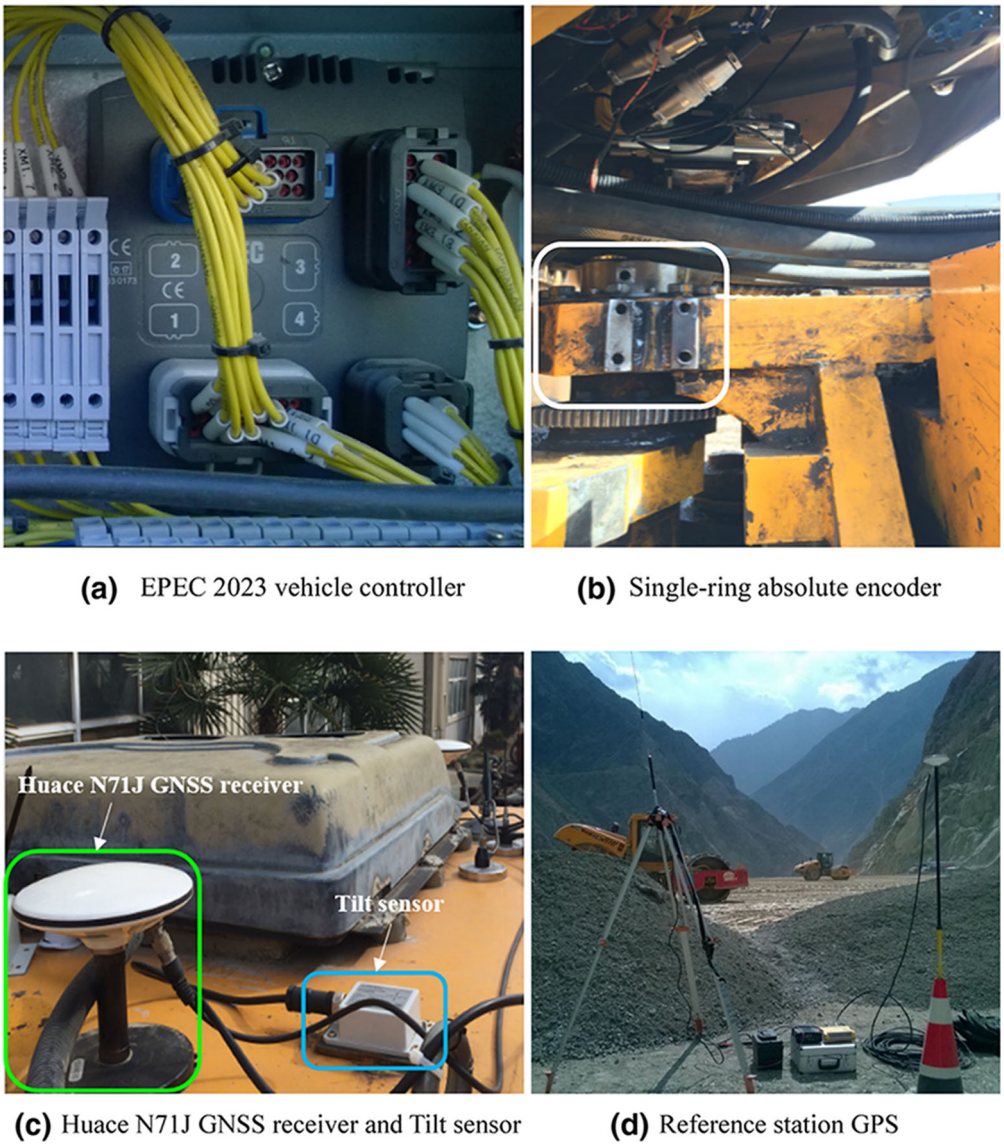


**Fig. 11** Experimental devices

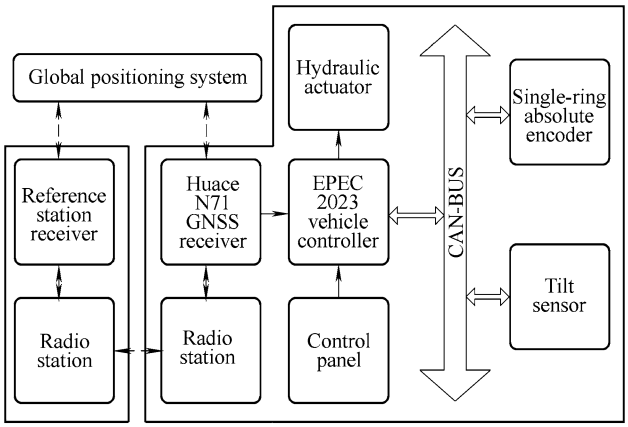


**Fig. 12** Structure diagram of the experimental setup

**Fig. 13** Experimental field

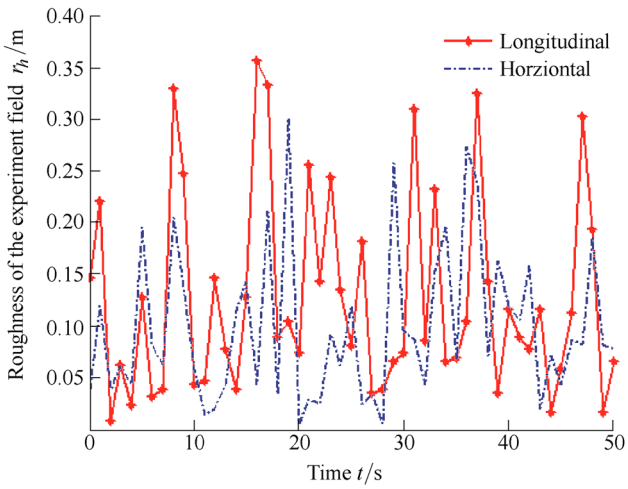


**Fig. 14** Roughness of the experiment field

difference between the actual displacement error and the calculated displacement error, protecting the experimental results from the effect of roughness.

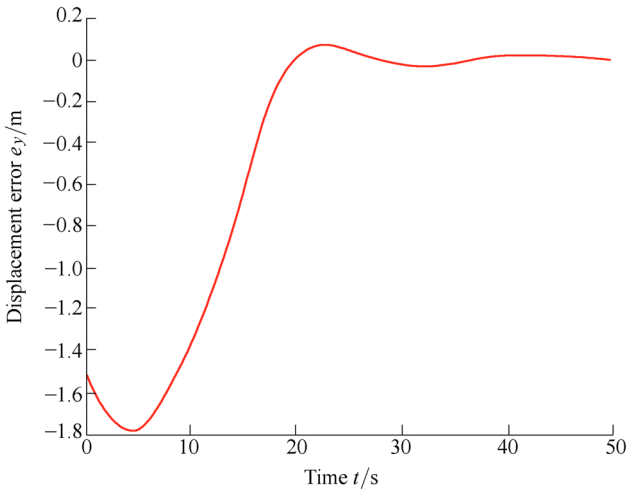


**Fig. 15** Experimental results of displacement error

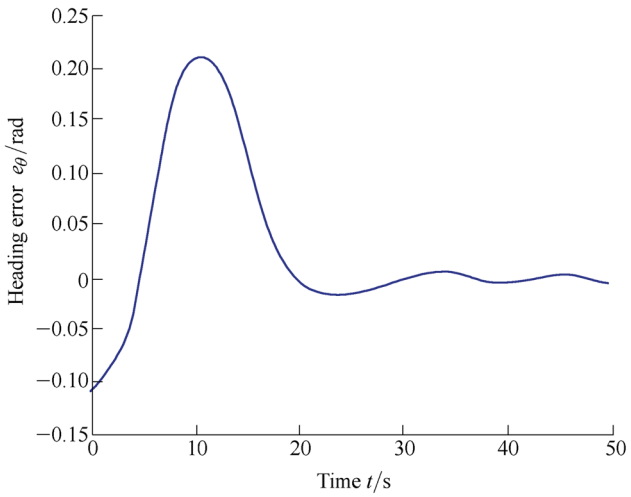


**Fig. 16** Experimental results of heading error

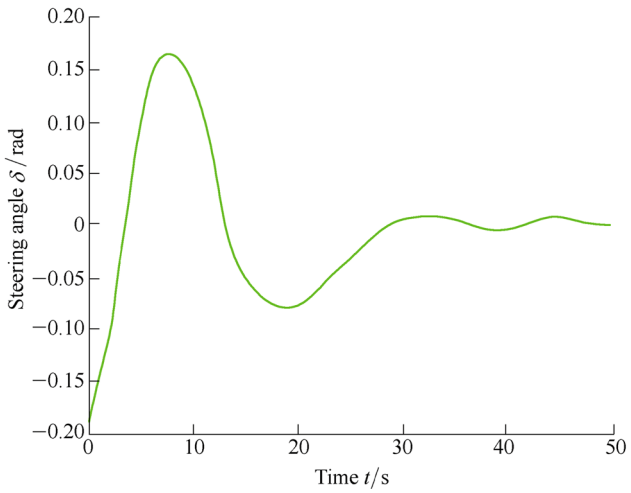


**Fig. 17** Experimental results of steering angle

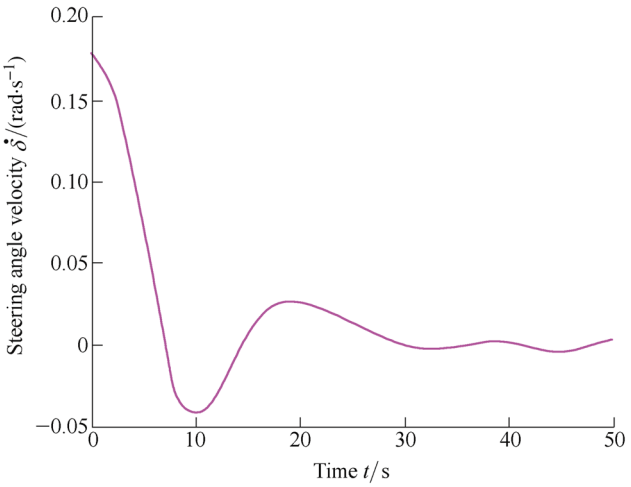


**Fig. 18** Experimental results of steering angle velocity

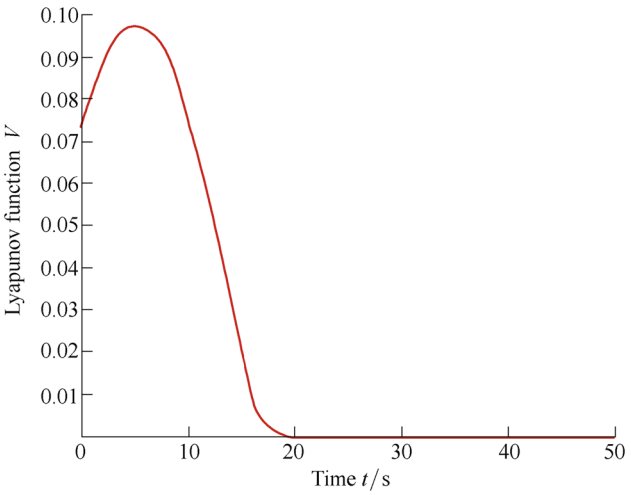


**Fig. 19** Experimental results of Lyapunov function

**Table 3** The parameters of the experimental results

| Parameter | Peak value | Peak time/s | Trough value | Trough time/s | Zero Time/s |
|---|---|---|---|---|---|
| Displacement error $e_y$ /m | 0.06 | 23 | −1.78 | 5 | 28 |
| Heading error $e_\theta$ /rad | 0.21 | 11 | −0.017 | 23 | 29 |
| Steering angle $\delta$ /rad | 0.165 | 8 | −0.081 | 19 | 35 |
| Steering angle velocity $\dot{\delta}$ /(rad·s$^{-1}$) | 0.027 | 19 | −0.041 | 10 | 29 |
| Lyapunov function $V$ | 0.097 | 5 | 0 | 19 | 19 |

However, compared with the simulation results, the experimental results might sometimes have a 1–4-second delay, which was mainly caused by the late response of steering system powered by hydraulic cylinders or the current resistance of rough field became bigger suddenly. But it didn't have much impact on the path following control.

From the above, it was shown that the articulated drum roller can lock into a desired path under a harsh environment like a construction site. Therefore, the proposed method is effective and practical.

## 7 Conclusions

(1) The linear mathematical error dynamic state-space equation, based on the kinematic model of an articulated drum roller from geometric consideration of the vehicle and its velocity constrains, is employed to develop a control law. The designed state-feedback control law, based on Lyapunov stability theory, is proved to achieve the purpose of control by the analysis of stability.

(2) The simulation under the MATLAB/Simulink is performed. The results show that the errors and steering angle decrease gradually, and converge to zero after 30 s even if given initial displacement error (−1.5m), heading error (−0.11rad) and steering angle (−0.19 rad). Meanwhile, the control input is not saturated.

(3) The experiments at the uneven construction site are performed. The positioning algorithm provides position and orientation of the roller drum axle midpoint precisely, and the method to correct the position errors reduces the effect of experimental field roughness to the path following control and experimental results effectively. The results of the experiment are quite similar with the simulation results. It is confirmed that an articulated drum roller can lock into a desired path with the proposed method in uneven fields.

## References

1. CHIANG K W, DUONG T T, LIAO J K. The performance analysis of a real-time integrated INS/GPS vehicle navigation system with abnormal GPS measurement elimination[J]. *Sensors*, 2013, 13(8): 10599–10622.
2. JIAN W U, LIU Y, WANG F, et al. Vehicle active steering control research based on two-DOF robust internal model control[J]. *Chinese Journal of Mechanical Engineering*, 2016, 29(4): 1–8.
3. GE Q S, GUO G, HUA R P. Dynamic mathematical model of steering and horizontal swing for articulated vehicles[J]. *Mining & Processing Equipment*, 2000, 28(6): 29–31. (in Chinese)
4. LARSSON J. Unmanned operation of load-haul-dump vehicles in mining environments[D]. örebro University, 2011.

5. LAVALLE S M. Motion planning[J]. *Robotics & Automation Magazine IEEE*, 2011, 18(1): 79–89.
6. BUNIYAMIN N, WAN NGAH W A J, SARIFF N, et al. A simple local path planning algorithm for autonomous mobile robots[J]. *International Journal of Systems Applications, Engineering & development*, 2011, 5(2): 151–159.
7. WU J, ZHAO Y, JI X, et al. Generalized internal model robust control for active front steering intervention[J]. *Chinese Journal of Mechanical Engineering*, 2015, 28(2): 285–293.
8. CORKE P, RIDLEY P. Load haul dump vehicle kinematics and control[J]. *Journal of Dynamic Systems Measurement & Control*, 2003, 125(1): 54–59.
9. ZHANG M, ZHOU J, JI Y, et al. Positioning method for automatic navigation of agricultural vehicle[J]. *Transactions of the Chinese Society of Agricultural Engineering*, 2009, 25(1): 74–77.
10. GOMEZGIL J, ALONSOGARCIA S, GÓMEZGIL F J, et al. A simple method to improve autonomous GPS positioning for tractors.[J]. *Sensors*, 2011, 11(6): 5630–5644.
11. NAYL T, NIKOLAKOPOULOS G, GUSTAFSSON T. Kinematic modeling and extended simulation studies of a load hull dumping vehicle under the presence of slip angles[C]//*The IASTED International Conference on Modelling, Simulation and Identification*, Pittsburgh, USA, November 7–9. 2011: 344–349.
12. ALTAFINI C. Some properties of the general n-trailer[J]. *International Journal of Control*, 2001, 74(4): 409–424.
13. MARTINEZ J L, MORALES J, MANDOW A, et al. Steering limitations for a vehicle pulling passive trailers[J]. *IEEE Transactions on Control Systems Technology*, 2008, 16(4): 809–818.
14. LAUMOND J P. Controllability of a multibody mobile robot[J]. *IEEE Transactions on Robotics & Automation*, 1994, 9(6): 755–763.
15. YOSHIMOTO T, KAIDA K, FUKAO T, et al. Backward path following control of an articulated vehicle[C]//*IEEE/SICE International Symposium on System Integration*, Kobe, Japan, December 15–17. 2013: 48–53.
16. YANG B, SHIM T, FENG N, et al. Path tracking control for backing-up tractor-trailer system via model predictive control[C]//*Control and Decision Conference*, Taiyuan, China, May 23–25. IEEE, 2012: 198–203.
17. KHALAJI A K, MOOSAVIAN S A A. Switching control of a tractor-trailer wheeled robot[J]. *Acta Press*, 2015, 30(2).
18. HUYNH V T, SMITH R, KWOK N M, et al. A nonlinear PI and backstepping-based controller for tractor-steerable trailers influenced by slip[C]//*IEEE International Conference on Robotics & Automation*, Saint Paul, MN, USA, May 14–18. 2012: 245–252.
19. TIAN J, CHEN Q Y, SONG Z P, et al. Stability analysis and trajectory tracking control of articulated heavy vehicles[C]//*International Conference on Intelligent Transportation, Big Data and Smart City*, Halong Bay, Vietnam, December 19–20. IEEE, 2015: 744–748.
20. YAMAKAWA J, WATANABE K, YASUDA Y. Turning characteristics of articulated tracked vehicles. Vehicle characteristics and steering performance[J]. *Transactions of the Japan Society of Mechanical Engineers*, 2001, 67(657): 1544–1551.
21. ALSHAER B J, DARABSEH T T, ALHANOUTI M A. Path planning, modeling and simulation of an autonomous articulated heavy construction machine performing a loading cycle[J]. *Applied Mathematical Modelling*, 2013, 37(7): 5315–5325.
22. NAYL T, NIKOLAKOPOULOS G, GUSTAFSSON T. On-Line path planning for an articulated vehicle based on Model Predictive Control[C]//*2013 IEEE International Conference on Control Applications (CCA),* Hyderabad, India, August 28–30. IEEE, 2013: 772–777.
23. NAYL T, NIKOLAKOPOULOS G, GUSTAFSSON T. Effect of kinematic parameters on MPC based on-line motion planning for an articulated vehicle[J]. *Robotics & Autonomous Systems*, 2015, 70(C): 16–24.
24. SHIROMA N, ISHIKAWA S. Nonlinear straight path tracking control for an articulated steering type vehicle[C]//*ICCAS-SICE, 2009*, Fukuoka, Japan, August 18–21. IEEE, 2009: 2206–2211.
25. RAINS G C, THAI C, FAIRCLOTH A G, et al. Technical note: evaluation of a simple pure pursuit path-following algorithm for an autonomous, articulated-steer vehicle[J]. *Applied Engineering in Agriculture*, 2014(30): 367–374.
26. DELROBAEI M, MCISAAC K A. Parking control of a center-articulated mobile robot in presence of measurement noise[C]//*2010 IEEE Conference on Robotics Automation and Mechatronics(RAM),* Singapore, June 28–30. IEEE, 2010: 453–457.
27. KOU W, LIU X H, CHEN W, et al. Path tracking control of the wheeled off-road articulated vehicle with actuator saturation[J]. *Metallurgical and Mining Industry*, 2015(9): 1030–1035.
28. FRANKLIN G F, POWELL D J, EMAMI-NAEINI A. Feedback control of dynamic systems[M]. 5th ed. NJ: Prentice hall, 2006.
29. SLOTINE J J E, LI W. Applied nonlinear control[M]. Englewood Cliffs, NJ: Prentice hall, 1991.



**Yongming BIAN,** born in 1965, is currently a professor and a PhD candidate supervisor in *School of Mechanical Engineering, Tongji University, China*. He received his doctor degree from *Tongji University, China*. His main research interest is real-time network control theory and hydromechatronics. E-mail:ymbianmail@163.com

**Meng YANG,** born in 1990, is currently a PhD candidate in *School of Mechanical Engineering, Tongji University, China*. His research interest is electrical control technology, control theory and hydromechatronics . Tel:+86-13162739906; E-mail:stek_young@163.com

**Xiaojun FANG,** born in 1990, is currently a PhD candidate in *School of Mechanical Engineering, Tongji University, China*. His main research interest is hydraulic control system and hydromechatronics. E-mail:xiaojun320@aliyun.com

**Xiahui WANG,** born in 1989, is currently a master candidate in *School of Mechanical Engineering, Tongji University, China*. His research interest is network control theory and hydromechatronics. E-mail:figomengnan@qq.com